THE ASTROPHYSICAL JOURNAL, 260:612–624, 1982 September 15

A STATISTICAL SURVEY OF LOCAL PLANETARY NEBULAE

C. T. DAUB
San Diego State University
Received 1981 September 25; accepted 1982 March 24

ABSTRACT

An empirically determined relation between the ionized masses of planetary nebulae and a particular function of observational quantities is used to derive distances to 299 primarily nearby planetary nebulae. These distances are used to investigate the scale height of the galactic distribution of planetaries (125 pc), the rate of formation of planetaries ($5 \pm 2 \times 10^{-3}$ PN kpc^{-3} yr^{-1}), and certain aspects of the evolution of the nebulae.

Subject heading: nebulae: planetary

I. INTRODUCTION

An essential requirement for an investigation of the statistics of planetary nebulae (PN) is a reliable distance scale. The classical method of deriving distances to large numbers of PN has been based on the assumption that each has approximately the same ionized mass (Shklovsky 1956*a*, *b*; O'Dell 1962; Seaton 1966; Cahn and Kaler 1971; Cudworth 1974; and others). This follows from the more general suppositions that PN have comparable total masses and that most of them are optically thin to Lyman continuous radiation from the central star. More recently Acker (1978) has computed distances to PN by utilizing a variety of methods: she assumed uniform masses for optically thin PN and uniform nebular luminosities for optically thick PN; additionally, her tabulation includes distances determined independently of astrophysical assumptions for certain individual PN. Although Acker's (1978) distances should be the most statistically reliable at this time; there are reasons for believing that her distances to optically thick nebulae have been inaccurately determined and that more trustworthy distances can be derived for them.

As Acker (1978) points out, Cudworth (1974) has concluded that the luminosity of a PN is not constant during the optically thick stage. Not only is the constant luminosity assumption central to Acker's (1978) distance computations for optically thick PN, but some of the criteria she uses for distinguishing the optically thick nebulae in the first place are based upon this assumption.

Recent work by Pottasch *et al.* (1978), Pottasch (1980), and Maciel and Pottasch (1980) has demonstrated that a large fraction of known PN are likely optically thick and, furthermore, a strong correlation exists between the nebular ionized mass and the nebular radius or density. This latter discovery leads to an alternative way of identifying and determining distances to the optically thick PN, which was first exploited by Maciel and Pottasch (1980).

In § II, after the derivation and discussion of pertinent physical relations, the ionized nebular mass is empirically related to a quantity derivable from observation. This relation is used in § III to derive distances to all PN with measured free-free radio fluxes and angular diameters; this then enables the local galactic distribution of PN to be examined. In § IV the frequency distribution of nebular radii is derived and discussed; conclusions about the formation rate of PN then follow. Some discussion regarding the luminosity evolution of PN comprises § V, and the paper concludes in § VI with a brief summary.

II. ANALYSIS

The radio free-free emission coefficient at frequency ν can be written (Oster 1961; Milne and Aller 1975)

$$j_\nu = 3.75\times 10^{-40} t^{-1/2} N_e \times \left\{ [N(\mathrm{H}^+) + N(\mathrm{He}^+)] \times \ln\left(\frac{4.95\times 10^{13} t^{3/2}}{\nu}\right) + 4N(\mathrm{He}^{++}) \times \ln\left(\frac{2.47\times 10^{13} t^{3/2}}{\nu}\right)\right\} \text{ ergs cm}^{-3}\text{ s}^{-1}\text{ Hz}^{-1}, \quad (1)$$

where N_e is the electron density (cm^{-3}); $N(\mathrm{H}^+)$, $N(\mathrm{He}^+)$, and $N(\mathrm{He}^{++})$ are the densities (cm^{-3}) of singly ionized H and singly and doubly ionized He, respectively, and t is the kinetic temperature in units of 10^4 K. Taking $N(\mathrm{He}^+)/N(\mathrm{H}^+) = N(\mathrm{He}^{++})/N(\mathrm{H}^+)$

$=0.06$ [and thus $\mathrm{Ne}=1.18N(\mathrm{H}^+)$] as being representative ionic abundances for PN and setting $\nu=5\times10^9$ Hz, a frequency at which many radio flux data are available and at which PN are expected to be optically thin, the emission coefficient becomes

$$j_{5\,\mathrm{GHz}}=3.75\times10^{-39}N_e^2 f(t)\ \mathrm{ergs\ cm^{-3}\ s^{-1}\ Hz^{-1}},\quad (2)$$

where $f(t)=t^{-1/2}(1+0.110\ln t^{3/2})$, a slowly varying function of temperature. After integrating the emission coefficient over the nebular volume, the flux at distance D (cm) from the nebula can be written as

$$F_{5\,\mathrm{GHz}}=\frac{\int j_{5\,\mathrm{GHz}}\,dV}{4\pi D^2}=\frac{3.75\times10^{-39}}{4\pi D^2}f(t)\int N_e^2\,dV\ \mathrm{ergs\ cm^{-2}\ s^{-1}\ Hz^{-1}},\quad (3)$$

where t is taken to be constant throughout the nebula.

The nebular ionized H mass is given by

$$M=1.67\times10^{-24}\int N(\mathrm{H}^+)\,dV=1.42\times10^{-24}\int N_e\,dV\,g.\quad (4)$$

It is convenient to define the "filling factor," ε, for the nebula as the ratio of the electron density averaged over the volume to the electron density averaged over the mass, i.e.,

$$\varepsilon=\frac{3\left(\int N_e\,dV\right)^2}{4\pi R^3\int N_e^2\,dV},\quad (5)$$

where R is the radius of the ionized portion. Equations (3), (4), and (5) can be combined to give

$$\frac{M^2 f(t)}{\varepsilon}=3.52\times10^{-9}F_{5\,\mathrm{GHz}}D^5\theta^3 g^2,\quad (6)$$

where $\theta=2R/D$ is the nebular angular diameter.

The quantity $[M^2 f(t)/\varepsilon]$ can be reliably evaluated for only those PN with accurately and independently determined distances. For this purpose Acker's (1978) compilation of distances to individual PN based on methods not requiring astrophysical assumptions (e.g., distances based on spectroscopic parallaxes of companion stars, a comparison of angular expansions with expansion velocities, kinematics, and interstellar extinction) and Khromov's (1979) list of expansion distances are used. To ensure accuracy, only PN with a spectroscopic parallax of a companion star or with at least two independent distance determinations all of which are within 20% of the mean of those distances are included. As it happened these stringent criteria eliminated all PN with expansion distances. Table 1 lists these mean distances for the 14 PN which meet the criteria and also tabulates

$$\log\left[\frac{M}{M_\odot}\left(\frac{f(t)}{\varepsilon}\right)^{1/2}\right]$$

as computed from equation (6); the requisite angular diameter and flux data are listed in Table 2 and are discussed in § III. Figure 1 illustrates the relation between

$$\frac{M}{M_\odot}\left[\frac{f(t)}{\varepsilon}\right]^{1/2}\quad\text{and}\quad\theta^2/S,$$

a function of observable quantities which is related to the nebular radius (see eqs. [9] and [12]); here $S=10^{23}F_{5\,\mathrm{GHz}}$, the flux at 5 GHz in janskys, and θ is the angular diameter, now and hereafter expressed in arcsec. It is apparent that the ionized mass increases by a large factor as the nebula expands and as, presumably, the degree of nebular optical thickness diminishes. The two mean lines in Figure 1 are drawn by eye estimate in order to more formally define the relation exhibited by the plotted points. These adopted mean lines differ little

TABLE 1

MASSES OF SELECTED PLANETARY NEBULAE

PN	D (pc)	$\mathrm{Log}\left[\frac{M}{M_\odot}\left(\frac{f(t)}{\varepsilon}\right)^{1/2}\right]$
NGC 40	1000[a,b]	−1.07
NGC 246	430[c]	−0.92
NGC 1514 ...	660[c]	−0.87
NGC 2452 ...	3000[a,d]	−0.70
NGC 2867 ...	1350[a,b]	−1.63
NGC 3132 ...	840[c]	−1.01
NGC 6567 ...	1000[a,d]	−2.09
NGC 6572 ...	680[a,b]	−1.87
NGC 6772 ...	1450[a,b]	−0.64
NGC 6804 ...	1350[a,b]	−0.69
NGC 6894 ...	1350[a,d]	−1.11
NGC 7026 ...	1780[a,d]	−0.79
IC 1747.......	2250[a,d]	−1.17
M1-59	1430[a,d]	−2.27

[a]Nebular extinction and a mean absorption law in the galactic disk.

[b]Nebular radial velocity and a model of galactic rotation.

[c]Spectroscopic parallax of a companion star.

[d]Nebular extinction compared with extinction of angularly nearby stars.

TABLE 2

CALCULATED DISTANCES AND RADII FOR PLANETARY NEBULAE

PK Number	PN	θ (arc sec)	S(Jy)	R(pc)	D(pc)	PK Number	PN	θ (arc sec)	S(Jy)	R(pc)	D(pc)
120 +9°1	NGC 40	38	.459[2]	.099	1070	341 +13°1	NGC 6026	54	.062[4]	.194	1480
118 -74°1	NGC 246	240	.247[4]	.268	460	64 +48°1	NGC 6058	25	.030[2]	.165	2720
130 -10°1	NGC 650-1	90	.110[2]	.223	974	342 +10°1	NGC 6072	60	.152[1]	.169	1160
220 -53°1	NGC 1360	500	.503[1]	.311	257	341 +5°1	NGC 6153	25	.477[1]	.058	960
144 +6°1	NGC 1501	58	.223[2]	.155	1100	336 -0°1	NGC 6164-5	370	2.5[4]	.200	223
165 -15°1	NGC 1514	120	.300[2]	.195	671	43 +37°1	NGC 6210	20	.311[1]	.058	1190
206 -40°1	NGC 1535	20	.172[4]	.082	1700	349 +1°1	NGC 6302	120	3.488[1]	.116	399
196 -10°1	NGC 2022	22	.091[4]	.126	2360	9 +14°1	NGC 6309	20	.151[1]	.089	1830
215 +3°1	NGC 2346	60	.086[1]	.190	1300	338 -8°1	NGC 6326	14	.073[1]	.090	2640
189 +19°1	NGC 2371-2	54	.090[2]	.180	1380	349 -1°1	NGC 6337	50	.103[1]	.170	1400
197 +17°1	NGC 2392	47	.251[4]	.139	1220	2 +5°1	NGC 6369	30	2.002[1]	.031	422
231 +4°2	NGC 2438	70	.094[1]	.198	1170	11 +5°1	NGC 6439	6	.050[1]	.041	2800
234 +2°1	NGC 2440	54	.422[4]	.132	1010	8 +3°1	NGC 6445	40	.368[1]	.120	1230
243 -1°1	NGC 2452	22	.055[1]	.139	2610	10 +0°1	NGC 6537	10	.671[1]	.016	652
239 +13°1	NGC 2610	40	.035[1]	.193	1990	96 +29°1	NGC 6543	22	.898[2]	.034	640
265 +4°1	NGC 2792	12	.122[1]	.055	1880	358 -7°1	NGC 6563	55	.077[1]	.187	1410
261 +8°1	NGC 2818	40	.033[1]	.196	2020	3 -4°5	NGC 6565	10	.040[1]	.086	3540
278 -5°1	NGC 2867	12	.252[1]	.035	1220	11 -0°2	NGC 6567	11	.176[1]	.040	1480
277 -3°1	NGC 2899	120	.086[1]	.251	860	34 +11°1	NGC 6572	15	1.307[1]	.017	474
272 +12°1	NGC 3132	64	.235[1]	.159	1030	10 -1°1	NGC 6578	8.5	.170[1]	.030	1440
296 -20°1	NGC 3195	40	.035[1]	.193	1990	5 -6°1	NGC 6620	5	.013[1]	.073	6050
286 -4°1	NGC 3211	14	.080[4]	.085	2500	9 -5°1	NGC 6629	16	.292[1]	.046	1180
261 +32°1	NGC 3242	42	.896[1]	.074	730	63 +13°1	NGC 6720	86	.365[2]	.164	790
148 +57°1	NGC 3587	200	.144[2]	.277	572	33 -2°1	NGC 6741	9	.220[1]	.027	1250
292 +1°1	NGC 3699	68	.067[1]	.210	1270	29 -5°1	NGC 6751	20	.063[1]	.130	2690
294 +4°1	NGC 3918	12	.859[1]	.017	583	33 -6°1	NGC 6772	70	.084[1]	.203	1200
298 -4°1	NGC 4071	75	.026[1]	.264	1450	34 -6°1	NGC 6778	19	.055[1]	.131	2850
294 +43°1	NGC 4361	82	.207[1]	.180	908	41 -2°1	NGC 6781	110	.390[1]	.179	671
307 -3°1	NGC 5189	170	.413[4]	.210	511	37 -6°1	NGC 6790	8.7	.256[1]	.024	1130
312 +10°1	NGC 5307	12.5	.095[1]	.067	2200	46 -4°1	NGC 6803	5.5	.114[1]	.022	1680
309 -4°2	NGC 5315	5	.480[4]	.008	694	45 -4°1	NGC 6804	63	.132[1]	.178	1160
331 +16°1	NGC 5873	3	.048[1]	.018	2490	42 -6°1	NGC 6807	2	.022[1]	.018	3670
327 +10°1	NGC 5882	7	.334[4]	.016	920	25 -17°1	NGC 6818	22	.281[1]	.069	1290
322 -5°1	NGC 5979	8	.117[1]	.034	1780	83 +12°1	NGC 6826	27	.405[2]	.070	1080

TABLE 2—*Continued*

PK Number	PN	θ (arc sec)	S(Jy)	R(pc)	D(pc)	PK Number	PN	θ (arc sec)	S(Jy)	R(pc)	D(pc)
82 +11°1	NGC 6833	2	.150[2]	.006	1160	123 +34°1	IC 3568	18	.075[2]	.119	2730
65 +0°1	NGC 6842	54	.128[2]	.168	1280	304 -4°1	IC 4191	14	.170[4]	.054	1590
42 -14°1	NGC 6852	28	.020[4]	.187	2760	319 +15°1	IC 4406	30	.110[1]	.137	1880
60 -3°1	NGC 6853	480	1.325[1]	.252	217	25 +40°1	IC 4593	13	.104[1]	.066	2100
57 -8°1	NGC 6879	5	.026[2]	.048	3990	0 +12°1	IC 4634	10	.129[1]	.042	1750
74 +2°1	NGC 6881	4	.131[2]	.014	1450	345 +0°1	IC 4637	21	.401[1]	.052	1030
82 +7°1	NGC 6884	6.5	.237[2]	.018	1120	334 -9°1	IC 4642	17	.060[4]	.123	2990
60 -7°2	NGC 6886	6	.105[1]	.026	1790	346 -8°1	IC 4663	14	.045[1]	.120	3530
54 -12°1	NGC 6891	15	.140[1]	.066	1810	3 -2°3	IC 4673	17	.036[1]	.136	3310
69 -2°1	NGC 6894	44	.056[2]	.183	1710	348 -13°1	IC 4699	7	.020[1]	.085	4990
61 -9°1	NGC 6905	46	.062[1]	.182	1630	10 -6°1	IC 4732	3	.056[1]	.017	2270
93 +5°2	NGC 7008	93	.280[2]	.179	793	2 -13°1	IC 4776	8	.067[1]	.048	2480
37 -34°1	NGC 7009	30	.750[1]	.055	759	58 -10°1	IC 4997	1.5	.127[1]	.004	1210
89 +0°1	NGC 7026	26	.302[2]	.080	1270	89 -5°1	IC 5117	2	.191[2]	.005	1000
84 -3°1	NGC 7027	17	6.947[2]	.007	178	100 -5°1	IC 5217	7	.130[2]	.028	1620
88 -1°1	NGC 7048	60	.140[2]	.172	1180	215 -30°1	A7	850	.305[4]	.426	207
66 -28°1	NGC 7094	98	.011[4]	.349	1470	196 -12°1	A11	30	.010[4]	.221	3040
104 +7°1	NGC 7139	82	.029[2]	.267	1350	198 -6°1	A12	37	.036[4]	.186	2080
36 -57°1	NGC 7293	900	1.292[1]	.326	150	204 -8°1	A13	150	.026[4]	.348	957
107 +2°1	NGC 7354	32	.598[2]	.068	881	197 -3°1	A14	40	.010[4]	.248	2560
106 -17°1	NGC 7662	30	.637[2]	.061	837	233 -16°1	A15	34	.022[4]	.199	2410
138 +2°1	IC 289	42	.214[2]	.137	1350	214 +7°1	A20	64	.014[4]	.280	1810
159 -15°1	IC 351	8	.051[2]	.057	2920	249 -5°1	A23	54	.010[4]	.280	2140
215 -24°1	IC 418	14	1.613[1]	.014	412	217 +14°1	A24	360	.055[4]	.425	487
25 -4°2	IC 1295	100	.049[1]	.261	1080	238 +34°1	A33	270	.022[4]	.455	695
130 +1°1	IC 1747	13	.128[2]	.058	1860	303 +40°1	A35	900	.255[4]	.451	207
161 -14°1	IC 2003	7	.044[2]	.053	3110	318 +41°1	A36	480	.215[4]	.363	312
169 -0°1	IC 2120	41	.096[3]	.160	1600	359 +15°1	A40	32	.007[4]	.244	3140
166 +10°1	IC 2149	15	.31[2]	.041	1120	25 -11°1	A60	80	.011[4]	.321	1660
221 -12°1	IC 2165	9	.188[1]	.030	1370	17 -21°1	A65	135	.011[1]	.396	1210
285 -14°1	IC 2448	9	.067[1]	.055	2540	19 -23°1	A66	270	.056[4]	.378	577
281 -5°1	IC 2501	2	.261[1]	.004	832	289 -0°1	AG Car	37	.285[1]	.123	1370
285 -5°1	IC 2553	4	.092[1]	.017	1790	3 -4°7	Ap 1-12	12	.013[4]	.146	5000
291 -4°1	IC 2621	5	.195[1]	.014	1190	35 -0°1	Ap 2-1	38	.220[5]	.131	1420

TABLE 2—*Continued*

PK Number	PN	θ (arc sec)	S(Jy)	R(pc)	D(pc)
171 -25°1	Ba 1	40	.013[1]	.239	2430
64 +5°1	BD 30°3639	12	.586[2]	.021	733
356 -4°1	Cn 2-1	2.5	.060[4]	.013	2100
38 +12°1	Cn 3-1	6	.055[1]	.038	2640
290 +7°1	Fg 1	30	.055[1]	.157	2160
352 +3°2	H 1-8	3.5	.031[4]	.028	3340
358 +3°6	H 1-20	4.5	.049[4]	.029	2670
5 +4°1	H 1-27	6.5	.027[4]	.065	4110
356 -4°2	H 1-41	12.5	.025[4]	.130	4280
357 -4°1	H 1-42	6	.040[4]	.046	3200
350 +4°1	H 2-1	5.5	.070[4]	.030	2250
3 +5°1	H 2-15	4.5	.010[4]	.076	6930
5 +5°2	H 2-16	16	.009[4]	.176	4530
3 +3°1	H 2-17	3.5	.013[4]	.048	5630
4 +1°1	H 2-24	6	.013[4]	.091	6270
4 +2°1	H 2-25	4.5	.016[4]	.057	5230
3 +4°4	H 2-41	8	.100[5]	.038	1960
3 +4°9	H 2-43	9	.025[5]	.100	4600
3 +2°1	Hb 4	6	.180[1]	.019	1300
359 -0°1	Hb 5	20	.548[1]	.041	845
7 +1°1	Hb 6	6	.235[1]	.016	1100
3 -14°1	Hb 7	4	.033[2]	.032	3310
264 -12°1	He 2-5	3	.029[4]	.025	3380
264 -8°1	He 2-7	49	.047[4]	.198	1660
261 +2°1	He 2-15	20	.105[4]	.111	2280
275 -4°2	He 2-21	2.5	.016[1]	.028	4650
278 -6°1	He 2-26	38	.036[1]	.188	2040
275 -2°1	He 2-28	10	.020[4]	.124	5120
275 -2°2	He 2-29	14	.024[4]	.137	4040
274 +2°2	He 2-35	5	.020[1]	.057	4670
279 -3°1	He 2-36	10	.090[4]	.053	2180
288 -5°1	He 2-51	12	.057[4]	.086	2970
289 +7°1	He 2-63	3	.012[1]	.042	5730
296 -3°1	He 2-73	4	.076[4]	.019	2010
300 -2°1	He 2-86	3.5	.125[4]	.012	1450
309 -4°1	He 2-99	20	.018[4]	.167	3450
311 +2°1	He 2-102	9	.033[4]	.085	3890
310 -2°1	He 2-103	20	.018[4]	.167	3450
308 -12°1	He 2-105	35	.014[4]	.220	2590
312 -1°1	He 2-107	10	.065[4]	.064	2650
318 +8°1	He 2-108	11	.033[4]	.108	4050
315 -0°1	He 2-111	30	.073[1]	.149	2040
319 +6°1	He 2-112	14.5	.082[1]	.087	2480
318 -2°1	He 2-114	30	.011[4]	.217	2985
321 +2°1	He 2-115	3	.156[4]	.009	1230
318 -2°2	He 2-116	45	.010[4]	.260	2390
321 +2°2	He 2-117	5	.267[4]	.012	987
317 -5°1	He 2-119	50	.094[4]	.173	1430
321 +1°1	He 2-120	30	.026[4]	.183	2510
323 +2°1	He 2-123	4.5	.110[4]	.018	1640
325 +3°1	He 2-129	1.5	.035[4]	.010	2620
315 -13°1	He 2-131	6	.325[1]	.013	909
323 -2°1	He 2-132	18	.025[4]	.150	3440
324 -1°1	He 2-133	4	.210[4]	.011	1090
320 -9°1	He 2-138	7	.076[1]	.038	2240
327 -1°1	He 2-140	2.5	.080[4]	.011	1770
325 -4°1	He 2-141	14	.051[1]	.111	3270
327 -2°1	He 2-142	3.5	.065[1]	.018	2140
327 -1°1	He 2-143	5	.120[4]	.019	1590
328 -2°1	He 2-146	20	.186[4]	.078	1620
333 +1°1	He 2-152	11	.196[4]	.037	1390
338 +5°1	He 2-155	14.5	.070[4]	.096	2730
331 -2°1	He 2-157	3	.030[4]	.024	3310
330 -3°1	He 2-159	10	.025[4]	.114	4690
331 -2°2	He 2-161	10	.032[4]	.098	4050
332 -3°1	He 2-164	16	.097[4]	.089	2290
335 -1°1	He 2-169	8	.128[4]	.033	1690
336 -5°1	He 2-186	3	.021[4]	.030	4100

1982ApJ...260..612D

TABLE 2—*Continued*

PK Number	PN	θ (arc sec)	S(Jy)	R(pc)	D(pc)	PK Number	PN	θ (arc sec)	S(Jy)	R(pc)	D(pc)
55 +2°1	He 2-432	5	.070[5]	.027	2200	16 -4°1	M 1-54	17	.038[4]	.135	3280
68 +1°2	He 2-453	24	.015[5]	.186	3200	22 -2°1	M 1-57	9.5	.065[4]	.060	2620
119 -6°1	Hu 1-1	5	.013[2]	.073	6040	22 -3°1	M 1-58	7	.060[4]	.044	2580
86 -8°1	Hu 1-2	5	.145[2]	.017	1420	23 -2°1	M 1-59	5	.140[1]	.018	1450
51 +9°1	Hu 2-1	3	.168[2]	.009	1180	50 +3°1	M 1-67	90	.237[1]	.182	836
190 -17°1	J 320	11	.031[1]	.112	4200	68 -0°1	M 1-75	20	.026[2]	.155	3210
194 +2°1	J 900	10	.121[1]	.044	1820	107 -2°1	M 1-80	8	.013[2]	.124	6380
252 +4°1	K 1-1	50	.011[5]	.266	2190	10 +18°2	M 2-9	30	.035[1]	.172	2370
346 +12°1	K 1-3	100	.009[4]	.366	1510	11 +6°1	M 2-15	6	.019[4]	.073	5000
223 -2°1	K 1-8	80	.066[4]	.225	1160	356 -5°2	M 2-24	11	.008[4]	.155	5810
236 +3°1	K 1-12	38	.010[4]	.243	2640	3 -6°1	M 2-36	9	.025[4]	.100	4600
204 +4°1	K 2-2	410	.054[4]	.450	452	8 -4°1	M 2-39	3.5	.008[4]	.064	7540
275 +72°1	K 2-4	774	.202[4]	.445	237	27 +0°1	M 2-45	7	.130[4]	.028	1630
39 +2°1	K 3-17	19	.450[5]	.043	940	39 -2°1	M 2-47	7.5	.078[4]	.041	2240
48 +2°1	K 3-24	6	.026[2]	.060	4140	242 -11°1	M 3-1	14	.024[1]	.137	4040
165 -6°1	K 3-67	15	.040[5]	.127	3490	221 +5°1	M 3-3	15	.130[5]	.069	1890
	K 3-77	7.5	.100[5]	.035	1930	241 +2°1	M 3-4	14	.016[4]	.149	4380
130 -11°1	M 1-1	6	.047[2]	.042	2900	245 +1°1	M 3-5	7	.024[4]	.076	4480
147 -2°1	M 1-4	4	.100[5]	.017	1700	254 +5°1	M 3-6	11	.105[4]	.054	2020
184 -2°1	M 1-5	7.5	.090[5]	.037	2060	357 +3°1	M 3-7	6.5	.028[4]	.063	4020
189 +7°1	M 1-7	9	.013[4]	.130	5950	358 +4°1	M 3-8	5.5	.027[4]	.053	3980
210 +1°1	M 1-8	22	.023[4]	.165	3100	359 +5°2	M 3-9	17	.031[4]	.141	3410
232 -1°1	M 1-13	10	.023[1]	.120	4930	358 +3°1	M 3-10	3.5	.020[4]	.037	4350
226 +5°1	M 1-16	3	.028[4]	.025	3450	5 +6°1	M 3-11	8	.025[5]	.087	4490
228 +5°1	M 1-17	3	.025[1]	.027	3690	5 +5°1	M 3-12	6.5	.040[5]	.051	3250
231 +4°1	M 1-18	33	.017[5]	.206	2580	355 -6°1	M 3-21	5	.030[1]	.044	3660
4 +4°1	M 1-25	5	.064[1]	.028	2320	0 -3°1	M 3-22	7.5	.020[5]	.092	5070
358 -0°2	M 1-26	4.5	.320[1]	.009	866	4 -11°1	M 3-29	8.5	.025[5]	.087	4490
6 +3°2	M 1-28	26	.020[4]	.182	2890	17 -4°1	M 3-30	17	.017[4]	.159	3850
8 -1°1	M 1-40	6	.250[4]	.015	1060	358 +5°1	M 3-39	20	.296[4]	.059	1220
2 -4°2	M 1-42	9	.030[4]	.090	4120	357 +3°2	M 3-41	4.5	.075[4]	.023	2070
16 -1°1	M 1-46	11	.095[1]	.057	2150	241 -7°1	M 4-1	5.5	.037[4]	.044	3290
14 -4°1	M 1-50	6	.050[4]	.041	2800	52 -2°2	Me 1-1	10	.035[4]	.093	3840
15 -4°1	M 1-53	6.5	.055[4]	.042	2680	342 +27°1	Me 2-1	7	.038[1]	.058	3400

1982ApJ...260..612D

TABLE 2—*Continued*

PK Number	PN	θ (arc sec)	S(Jy)	R(pc)	D(pc)
283 +2°1	My 60	7.5	.060[1]	.048	2620
307 -4°1	My Cn 18	6	.106[4]	.026	1780
322 -2°1	Mz 1	30	.061[1]	.154	2120
329 -2°2	Mz 2	28	.075[1]	.144	2120
331 -1°1	Mz 3	35	.649[1]	.072	854
263 -5°1	PB 2	3	.040[1]	.020	2780
269 -3°1	PB 3	7	.070[4]	.040	2360
275 -4°1	PB 4	10	.071[1]	.061	2510
278 +5°1	PB 6	11	.030[1]	.114	4290
292 +4°1	PB 8	5	.026[4]	.048	3990
336 -6°1	PC 14	7	.030[4]	.066	3920
288 -2°1	Pe 1-3	8	.024[4]	.089	4600
336 +1°1	Pe 1-6	10	.040[4]	.086	3540
25 -2°1	Pe 1-15	5	.030[5]	.044	3660
28 -4°1	Pe 1-20	7.5	.050[5]	.053	2930
28 -3°1	Pe 1-21	10	.030[5]	.102	4210
322 -0°1	Pe 2-8	1.5	.100[4]	.005	1400
36 -1°1	Sh 2-71	155	.083[1]	.280	744
195 -0°1	Sh 2-266	80	.159[1]	.188	971
329 +2°1	Sp 1	76	.075[4]	.214	1160
342 -14°1	Sp 3	35	.061[4]	.164	1930
345 -8°1	Tc 1	10	.801[1]	.014	586
306 -0°1	Th 2-A	24	.060[4]	.141	2430
197 -2°1	VV 1-4	130	.354[1]	.195	619
196 -1°1	VV 1-5	310	.642[1]	.245	326
235 +1°1	VV 1-7	270	.057[1]	.376	575
205 +14°1	YM 29	615	.327[4]	.369	247

NOTE.—Radio flux sources: (1) Milne and Aller 1975. (2) Cahn 1976. (3) Khromov 1979. (4) Milne 1979. (5) Cahn and Rubin 1974.

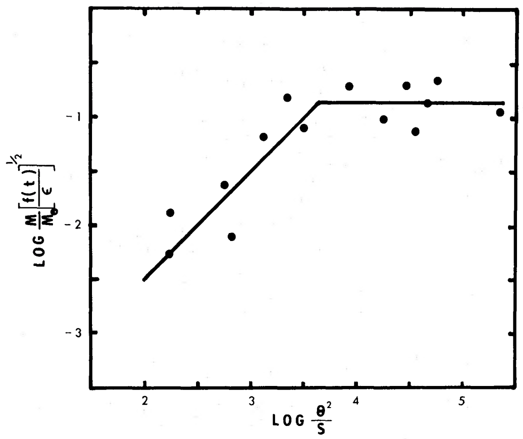

FIG. 1.—The relation between what is essentially the nebular ionized mass and the observed quantity θ^2/S; *dots*: The individual nebulae listed in Table 1; *lines*: The adopted mean relations expressed by eqs. (7) and (10).

from relations obtained by a least-squares analysis, and they have some advantage in simplicity over a more sophisticated approach. A similar plot of all PN with individually determined distances shows very large scatter but yields comparable results if median values of

$$\log\left[\frac{M}{M_\odot}\left(\frac{f(t)}{\varepsilon}\right)^{1/2}\right]$$

within various intervals of θ^2/S are computed. The equations of the two mean lines, the resultant nebular distance derived from equation (6), and the nebular radius are given by, for $\log(\theta^2/S) < 3.65$:

$$\log\left\{\frac{M}{M_\odot}\left[\frac{f(t)}{\varepsilon}\right]^{1/2}\right\} = \log\frac{\theta^2}{S} - 4.50, \tag{7}$$

$$D = 324\left(\frac{\theta}{S^3}\right)^{1/5}\ \mathrm{pc}, \tag{8}$$

$$R = 7.85\times10^{-4}\left(\frac{\theta^2}{S}\right)^{3/5}\ \mathrm{pc}, \tag{9}$$

and for $\log(\theta^2/S) > 3.65$:

$$\log\left\{\frac{M}{M_\odot}\left[\frac{f(t)}{\varepsilon}\right]^{1/2}\right\} = -0.85 \tag{10}$$

$$D = \frac{9300}{(\theta^3 S)^{1/5}}\ \mathrm{pc}, \tag{11}$$

$$R = 2.26\times10^{-2}\left(\frac{\theta^2}{S}\right)^{1/5}\ \mathrm{pc}. \tag{12}$$

Equations (7) and (9) lead, incidentally, to a relation between ionized mass and radius which is virtually indistinguishable from the mean relation between these parameters found by Pottasch (1980) if his values of t and ε are selected.

From equation (9) or equation (12) one notes that $R = 0.12$ pc when $\log\theta^2/S = 3.65$; this then would be the typical radius of a PN when it first becomes optically thin. The uncertainty in this determination of the transition radius is probably about 0.02 pc.

III. DISTANCES AND GALACTIC DISTRIBUTION

a) *Distances*

Table 2 lists 299 PN for which the required data are available. The angular diameters in the third column have been obtained primarily from Perek and Kohoutek (1967). If a nebula does not appear circularly symmetric, the largest dimension is adopted for the angular diameter; this is done in hopes of minimizing the effect of projection on the adopted angular dimension. Radio fluxes, listed in the fourth column, are taken from the compilations of Cahn and Rubin (1974), Cahn (1976), Milne and Aller (1975), and Milne (1979); one radio flux measurement is obtained from Khromov (1979). If an available flux measurement is at a frequency other than 5 GHz, an adjustment of that flux to $\nu = 5$ GHz was made using equation (1). The fifth column tabulates the nebular radii computed from equation (9) or equation (12); the sixth column tabulates the distances computed from equation (8) or equation (11).

The distances derived for the 122 optically thin nebulae ($\log\theta^2/S > 3.65$) are, of course, approximately the same as those determined by other investigators using the Shklovsky method. It is possible that some of the most expanded PN become optically thick for a second time as their central stars contract to near white dwarf dimensions, thereby resulting once again in a smaller ionized nebular mass (Seaton 1966); however, it is expected that a very small fraction of these PN should be affected by this, and the effect is ignored here.

The 177 optically thick PN ($\log\theta^2/S < 3.65$) have computed distances which are smaller than the Shklovsky method distances. From Figure 1 it is apparent that the most compact PN are likely to have ionized masses smaller by about a factor of 100 in comparison to a typical optically thin PN; hence, their derived distances will be a factor of 10 or so smaller than the distance computed on the basis of assuming a "normal" ionized mass.

It should be noted that the distances derived here often differ significantly from those of Maciel and Pottasch (1980), who also computed distances to some of the same PN allowing for a diminished ionized mass due to optical thickness. They used an empirically determined linear relation of the form $M = aR + b$ to relate mass and radius. This relationship leads to similar distances to those derived here except for the very small PN and the very large PN. The use of the linear relation leads to overestimates of the distances to large PN because it allows the mass to increase indefinitely with radius without an optically thin cut-off. For small PN the linear relation with $b<0$ does not enable a physically real distance to be derived or it leads to an overestimate of the distance relative to the distance scale found here.

b) *Galactic Distribution*

The investigation of the distribution of PN perpendicular to the galactic plane is made complicated by incompleteness effects; an attempt is made here to correct for incompleteness in an empirical manner.

Cahn and Wyatt (1976) find, for the nearby faint PN they investigated, a north-south asymmetry in equatorial coordinates. They concluded that a deeper and more thorough search of northern declination skies had led to a relative deficiency in the known number of such PN with negative declinations. This list of 299 PN, broken down into size and distance subsets, has also been examined for possible incompleteness due to surveying and/or observational biases. A definite directional asymmetry is found only for more distant PN which, however, seems fully explainable by the galactic radial density gradient. No correction is therefore made for directionally dependent incompleteness. Some care is taken in what follows to allow for the effects of distance dependent incompletion.

If it is assumed that the number density of local PN is uniform in the galactic plane and as a function of distance z from the galactic plane is given by the exponential law,

$$\rho=\rho_0 e^{-kz}, \tag{13}$$

then it is easy to derive the density projected onto the galactic plane

$$\rho_1=\frac{2\rho_0}{k}, \tag{14}$$

the number N of PN closer than distance D from an observer at $z=0$

$$N=2\pi\rho_0\left[\frac{D^2}{k}-\frac{2}{k^3}+e^{-kD}\left(\frac{2D}{k^2}+\frac{2}{k^3}\right)\right], \tag{15}$$

and the fraction f_z of all PN which are within distance z of the galactic plane

$$f_z=1-e^{-kz}. \tag{16}$$

A perusal of the compilation of nebular distances and radii given in Table 2 indicated that the discovery of most PN might be essentially complete to a distance somewhat beyond 1 kpc; large PN, however, are less evidently complete to that distance. To investigate this more formally, the 266 PN with $R<0.24$ pc were selected, and equation (15) was used to compute ρ_0 for regions at successive distance intervals of 100 pc. As an example, the number of these PN with 800 pc $<D<$ 900 pc is seven. Writing equation (15) once for $D=800$ pc and again for $D=900$ pc, then subtracting these equations and taking $k=8$ kpc^{-1}, yields $\rho_0=52.5$ kpc^{-3}. Figure 2 plots the other computed values of ρ_0 and

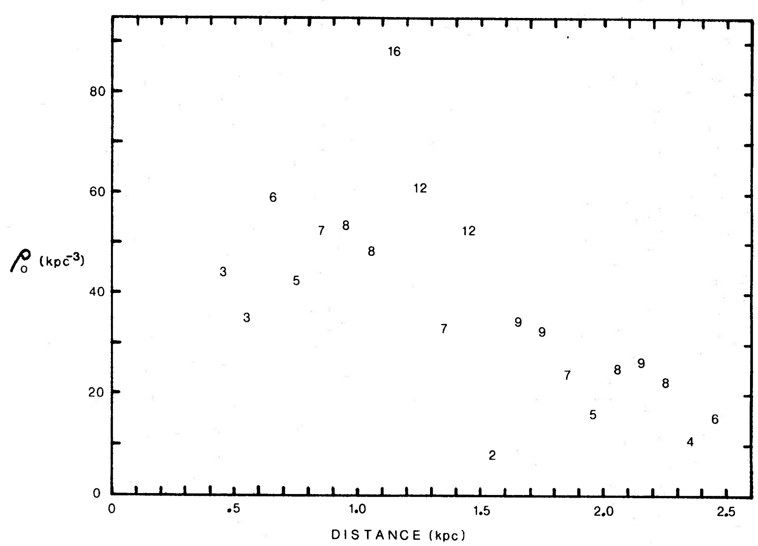

FIG. 2.—The computed galactic plane density of PN whose radii are smaller than 0.24 pc plotted vs. distance. The observed number of PN within each 100 pc distance interval is indicated. The actual galactic plane density of these PN is apparently about 55 kpc^{-3}; the diminishing densities derived for distances beyond about 1.5 kpc are attributed to incompleteness.

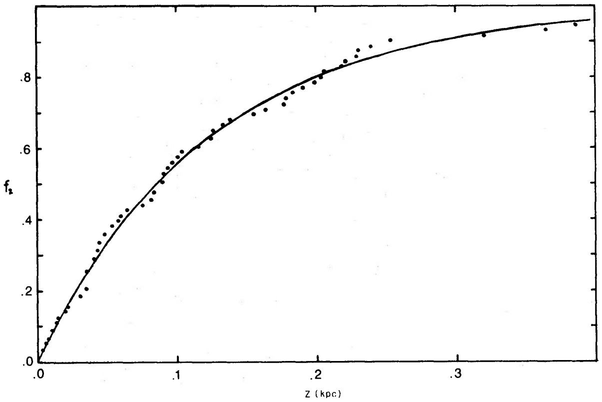

FIG. 3.—The fraction of PN which are within distance z of the galactic plane. *Dots*: The observed distribution for PN with radii smaller than 0.24 pc and distances less than or equal to 1.25 kpc; *line*: An exponential distribution corresponding to a scale height of 125 pc.

indicates the counts of PN within 100 pc intervals of distance from 400 pc to 2500 pc. Very similar results were obtained for other values of k between 5 kpc^{-1} and 15 kpc^{-1}. On the basis of Figure 2 it is apparent that this sample of PN is essentially complete out to a distance of about 1.25 kpc and, as will be of interest later, ρ_0 for PN with $R < 0.24$ pc is approximately 55 kpc^{-3}.

Selecting the 67 PN of this sample whose distances are less than or equal to 1.25 kpc, the fraction of these which are within distance z of the galactic plane may be computed as a function of z; in doing this, half of each PN is considered to be within its computed z distance and half beyond that distance. Figure 3 shows the relation found by this procedure. The solid curve in Figure 3 is the expected f_z versus z relation computed from equation (16) with $k = 8$ kpc^{-1}. The very close agreement between the theoretical curve and the plotted points indicates that the assumed exponential law quite closely represents the distribution of PN and that the scale height is given adequately by $k^{-1} = 125$ pc. This differs little from previous derivations of this quantity (e.g., Cahn and Kaler 1971), and it is similar to the scale height of main sequence stars of approximately 2 $M_\odot$ (Allen 1973).

IV. DISTRIBUTION OF RADII AND FORMATION RATE

A histogram of the frequency of occurrence of PN radii is shown in Figure 4*a*. Figure 4*b* is a similar histogram for the 54 PN within 1000 pc. It should be less affected by incompleteness. An attempt is also made to correct the observed number of PN within various radii intervals for the effects of incompleteness. For this purpose, nebulae within each 0.02 pc radius interval, or larger interval if necessary to give a minimum of about 30 PN, were considered separately. Equation (15), with

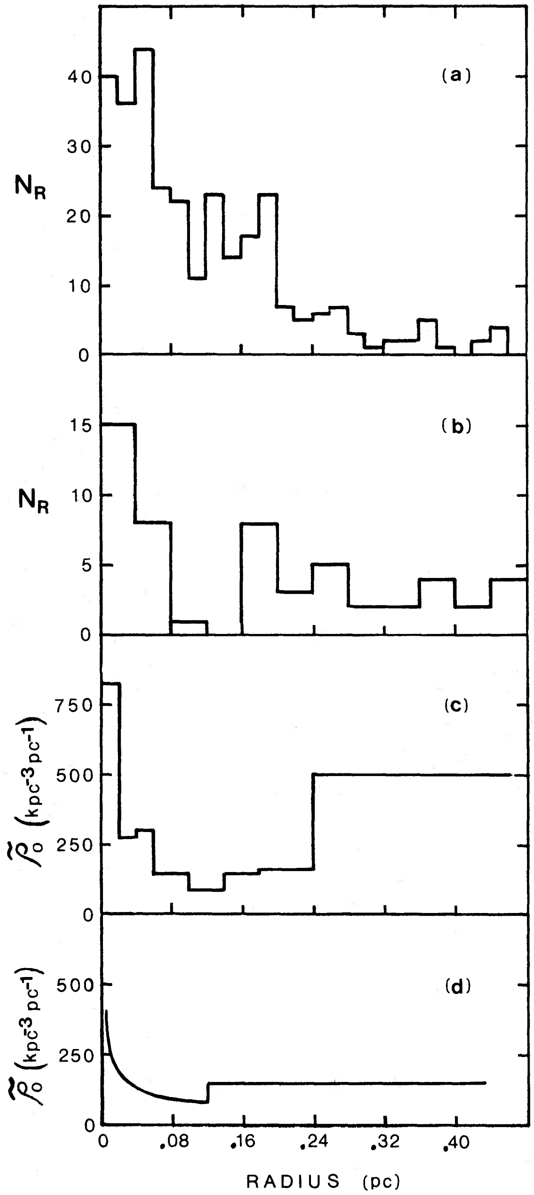

FIG. 4.—(*a*) For all 299 PN, the number within each 0.02 pc radius interval. (*b*) For the 54 PN closer than 1000 pc, the number within each 0.04 pc radius interval. (*c*) The galactic plane density of PN as a function of nebular radius after correcting for incompleteness. (*d*) The distribution of nebular radii expected from a simple theory of uniformly expanding PN.

$k = 8$ kpc^{-1}, was used to compute ρ_0 versus D out to each successive PN arranged in order of distance. In doing this, each PN was again considered to be "smeared out" such that half of it was closer than its computed distance and half of it farther away. For example, for the closest PN in the radius interval 0 pc $< R <$ 0.02 pc, $D = 0.178$ kpc and $N = 1.5$ yielding $\rho_0 = 34.1$ kpc^{-3} from equation (15). Figure 5 plots the computed values

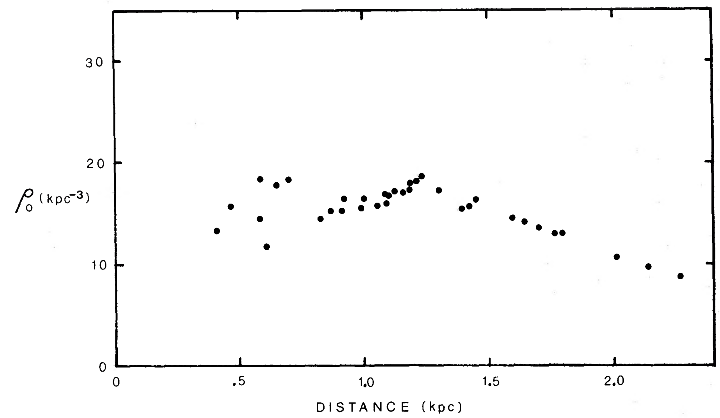

FIG. 5.—The galactic plane density of PN with radii smaller than 0.02 pc which is implied by the number of such PN which are closer than distance D. The densities are computed from eq. (15) with $k = 8$ kpc^{-1}. The graph indicates that knowledge of the presence of these small PN is essentially complete out to somewhat beyond 1 kpc and that a reasonable estimate of ρ_0 for these PN is 16.5 kpc^{-3}.

of ρ_0 versus D for $N = 0.5$ to 35.5 (the 36 PN in this size range out to slightly beyond 2 kpc) in unit steps of N. An examination of the distribution of the plotted points suggests $\rho_0 \approx 16.5$ for PN in the smallest radius interval; normalizing to a 1 pc radius interval gives $\tilde{\rho}_0 \approx 825$ kpc^{-3} pc^{-1}. This procedure is repeated to determine approximate values of $\tilde{\rho}_0$ for nebulae in other radius intervals. Figure 4c displays the resultant histogram which should, then, approximately represent the true radius distribution of PN.

It is curious that the greatest frequency of occurrence is for the very small and the very large PN; there is also a definite minimum in the number of PN near $R = 0.12$ pc.

An attempt was made to reproduce the observed size distribution by constructing a simple model for an expanding PN. Figure 4d illustrates the expected size distribution, normalized to $\tilde{\rho}_0 = 150$ PN kpc^{-3} pc^{-1} as found for optically thin nebulae with $R < 0.24$ pc, of the ionized Strömgren zones of uniform density PN with nonvariable central stars. It is also assumed that the nebulae have constant total mass, have outer surfaces which expand at constant velocity, and become optically thin at a radius of 0.12 pc. The large number of PN at small radii is a consequence of an initially small ionization front velocity. With declining density, the velocity of the front increases so fewer PN are predicted to have the larger radii. Just before the transition to optical thinness, the ionization front velocity is twice the expansion velocity of the medium; hence the discontinuity at a radius of 0.12 pc, where the expected number of PN per unit radius interval doubles. The similarity of the theoretical distribution to the observed distribution for PN with $R < 0.24$ pc is evident. Furthermore, this simple model is consistent with the observation that among the higher surface brightness PN, expansion velocity increases with radius (Bohuski and Smith 1974). It does seem, however, that the simple theoretical model predicts too few of the smallest PN and far too few PN with $R > 0.24$ pc. Factors which might improve the agreement are continuous or episodic mass loss from the central stars of the smallest, hence youngest, PN, thereby increasing the time during which the ionized radius is small, and diminished expansion velocities for the largest PN due to friction with the interstellar medium, hence leading to a relatively larger number of these PN. Other factors undoubtedly of importance in modeling the size distribution are nebular radial density gradients and a changing luminosity of stellar ionizing photons during the optically thick stage (see § V). In any case, the appearance of the size distribution histogram and its approximate similarity to the predictions of the simple model for an expanding PN give confidence in the essential correctness of the distance scale used here.

The rate of formation of PN in the galactic plane is given by

$$r(\mathrm{kpc}^{-3}\,\mathrm{yr}^{-1}) = 1.02\times10^{-6}\tilde{\rho}_0(\mathrm{kpc}^{-3}\,\mathrm{pc}^{-1})\,v(\mathrm{km\,s}^{-1}), \quad (17)$$

where v is the velocity of the ionization front for optically thick nebulae, and for optically thin nebulae it is the velocity of the outer boundary of nebular material. From Figure 4c, $\tilde{\rho}_0 \approx 155$ kpc^{-3} pc^{-1} for optically thin nebulae smaller than 0.24 pc in radius. The area under the histogram in Figure 4c gives a total density in the galactic plane for all PN with $R < 0.24$ pc of 53 kpc^{-3}, or $\tilde{\rho}_0 = 220$ kpc^{-3} pc^{-1}. Especially uncertain is the parameter v. Cahn and Wyatt (1976) present arguments for taking $v = 20$ km s^{-1}, whereas Smith (1976) suggests $v = 30$ km s^{-1} as a *low* estimate. Therefore, a rather uncertain formation rate in the range $5 \pm 2 \times 10^{-3}$ PN

$\mathrm{kpc}^{-3}\ \mathrm{yr}^{-1}$ seems to be indicated. This rate is virtually identical to that found by Cahn and Wyatt (1976) and is comparable to the rate of formation of white dwarfs given by Weidemann (1977) of $2^{+2}_{-1}\times10^{-3}$ WD $\mathrm{kpc}^{-3}\ \mathrm{yr}^{-1}$.

It is also of interest to estimate the number of PN in the Galaxy. The derivation of this quantity is clearly dependent upon the nebular radius interval being considered and assumed galactic parameters. The radius range 0 pc to 0.24 pc is selected to avoid dealing with the smallness of the statistical sample of large PN. The surface density of PN with $R<0.24$ pc is found from equation (14) to be $\rho_1=13\ \mathrm{kpc}^{-2}$. If the local mass density projected onto the galactic plane is 0.019 g cm^{-2} (Allen 1973) and the number of PN per unit mass is constant in the Galaxy, then there are about 14000 PN per $10^{-11}\ M_{\odot}$.

V. LUMINOSITY EVOLUTION

The value of the luminosity of PN at 5 GHz is given by $4\pi D^2F_{5\ \mathrm{GHz}}$ which is, using equations (8) and (9) or equations (11) and (12) and recalling that $S=10^{23}F_{5\ \mathrm{GHz}}$,

$$L_{5\ \mathrm{GHz}}=1.37\times10^{21}R^{1/3}\ (\mathrm{pc})\ \mathrm{ergs\ s^{-1}\ Hz^{-1}} \quad \text{for } R<0.12\ \mathrm{pc}, \tag{18}$$

or

$$L_{5\ \mathrm{GHz}}=\frac{1.19\times10^{18}}{R^3\ (\mathrm{pc})}\ \mathrm{ergs\ s^{-1}\ Hz^{-1}} \quad \text{for } R>0.12\ \mathrm{pc}. \tag{19}$$

Figure 6 illustrates this luminosity-radius dependence. It is evident that there is a significant increase in luminosity during the optically thick stage; equation (18) predicts a 1.2 mag difference between the smallest ($R\approx0.005$ pc) and the largest ($R\approx0.12$ pc) of the optically thick PN. The peak 5 GHz luminosity at $R=0.12$ pc predicted by equations (18) or (19) is 7×10^{20} ergs $\mathrm{s^{-1}\ Hz^{-1}}$.

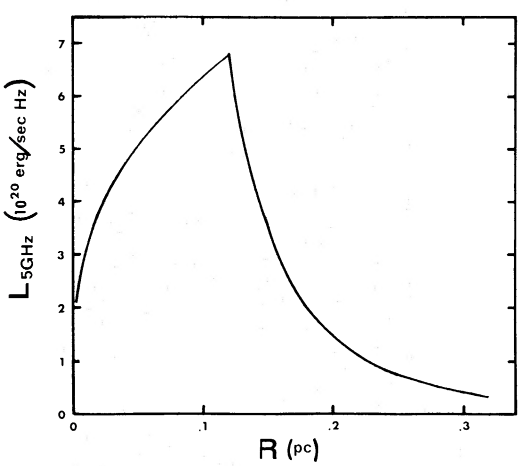

FIG. 6.—The nebular luminosity at 5 GHz vs. nebular radius which follows from the adopted relation between $M[f(t)/\varepsilon]^{1/2}$ and θ^2/S expressed by eqs. (7) and (10) and shown in Fig. 1.

If there is one ionization of H for each Lyman continuum photon emitted by the central star, then the number of Lyman continuum photons Q emitted is (Osterbrock 1974)

$$Q=2.60\times10^{-13}g(t)\int Ne^2\,dV\ \mathrm{s}^{-1}, \tag{20}$$

where $g(t)$ is a slowly varying function of temperature and $g(1)=1$. Using equation (2),

$$L_{5\ \mathrm{GHz}}=3.75\times10^{-39}f(t)\int Ne^2\,dV\ \mathrm{ergs\ s^{-1}\ Hz^{-1}}. \tag{21}$$

Combining equations (20) and (21) and taking $g(t)/f(t)=1$ gives the proportional relation:

$$Q=6.9\times10^{25}L_{5\ \mathrm{GHz}}. \tag{22}$$

Thus a nebular 5 GHz luminosity of 7×10^{20} ergs $\mathrm{s^{-1}\ Hz^{-1}}$ corresponds to 5×10^{46} stellar Lyman continuum photons s^{-1}. The increasing nebular 5 GHz luminosity during the optically thick stage, which is a consequence of the empirical relation shown in Figure 1, implies a steadily increasing emission of stellar Lyman continuum photons. This, of course, does not necessarily require that the stellar luminosity be increasing; in fact, the results here are qualitatively and approximately quantitatively consistent with early central star evolution at constant luminosity but increasing effective temperature as described by Pottasch *et al.* (1978).

VI. SUMMARY

Distances and radii of 299 PN have been computed after making allowances for the incomplete ionization of the nebular mass for that majority of PN which are optically thick in the Lyman continuum. For many of these radiation bounded PN, the derived distances and radii are significantly smaller than previously published values. Despite this, the distribution of PN perpendicular to the galactic plane (scale height ~ 125 pc) does not differ significantly from that found by others. The size distribution for PN is derived by correcting the "raw" size distribution for incompleteness within each nebular radius interval. This "true" radius distribution differs markedly from any previously derived radius distribution for PN but it seems interpretable, at least to first order, on the basis of a simple model of nebular expansion. The radius distribution also leads to an estimate for the galactic plane formation rate of PN of $5 \pm 2 \times 10^{-3}$ kpc^{-3} yr^{-1}, which is comparable to estimates of the formation rate of white dwarfs. Finally, a significant increase in the 5 GHz luminosity during the optically thick stage is demonstrated to also be a consequence of the adopted distance scale.

I thank William Kovach for valuable discussions and, especially, Julius Cahn for much valued help and advice.

REFERENCES

Acker, A. 1978, *Astr. Ap. Suppl.*, **33**, 367.
Allen, C. W. 1973, *Astrophysical Quantities* (3d ed.; London: Athlone Press).
Bohuski, T. J., and Smith, M. G. 1974, *Ap. J.*, **193**, 197.
Cahn, J. H. 1976, *A.J.*, **81**, 407.
Cahn, J. H., and Kaler, J. B. 1971, *Ap. J. Suppl.*, **22**, 319.
Cahn, J. H., and Rubin, R. H. 1974, *A.J.*, **79**, 128.
Cahn, J. H., and Wyatt, S. P. 1976, *Ap. J.*, **210**, 508.
Cudworth, K. M. 1974, *A.J.*, **79**, 1384.
Khromov, G. S. 1979, *Astrofizika*, **15**, 179.
Maciel, W. J., and Pottasch, S. R. 1980, *Astr. Ap.*, **88**, 1.
Milne, D. K. 1979, *Astr. Ap. Suppl.*, **36**, 227.
Milne, D. K., and Aller, L. H. 1975, *Astr. Ap.*, **38**, 183.
O'Dell, C. R. 1962, *Ap. J.*, **135**, 371.
Oster, L. 1961, *Rev. Mod. Phys.*, **33**, 525.
Osterbrock, D. E. 1974, *Astrophysics of Gaseous Nebulae* (San Francisco: Freeman), p. 17.
Perek, L., and Kohoutek, L. 1967 *Catalogue of Galactic Planetary Nebulae* (Prague: Academia).
Pottasch, S. R. 1980, *Astr. Ap.*, **89**, 336.
Pottasch, S. R., Wesselius, P. R., Wu, C.-C., Fieton, H., and Van Duinen, R. J. 1978, *Astr. Ap.*, **62**, 95.
Seaton, M. J. 1966, *M.N.R.A.S.*, **132**, 113.
Shklovsky, I. S. 1956*a*, *Astr. Zh.*, **33**, 222.
______. 1956*b*, *Astr. Zh.*, **33**, 315.
Smith, H., Jr. 1976, *Astr. Ap.*, **53**, 333.
Weidemann, V. 1977, *Astr. Ap.*, **61**, L27.

C. T. DAUB: Astronomy Department, San Diego State University, San Diego, CA 92182